



Search for Neutral Higgs Bosons at High $\tan\beta$ in the $b(h/H/A) \rightarrow b\tau^+\tau^-$ Channel

The DØ Collaboration
URL <http://www-d0.fnal.gov>
(Dated: July 25, 2006)

A search for the production of neutral Higgs bosons in association with bottom quarks in $p\bar{p}$ collisions at $\sqrt{s} = 1.96$ TeV is presented. The cross section for this process is enhanced in many extensions of the Standard Model (SM), such as in its Minimal Supersymmetric extension (MSSM) at large $\tan\beta$. The search is performed using the decay of the Higgs boson into two τ -leptons. The data, corresponding to an integrated luminosity of 344 pb^{-1} , were collected with the DØ detector at the Fermilab Tevatron Collider. The results provide an upper limit for the production cross section of neutral Higgs bosons in the mass range of 90 to 150 GeV, and are interpreted in the MSSM. This cross section limit is competitive with the one obtained previously using the decay of the Higgs into two b -quarks, despite the 1:9 branching ratio of the $\tau^+\tau^-$ to $b\bar{b}$ decay modes.

I. INTRODUCTION

In the Minimal Supersymmetric extension of the Standard Model (MSSM), the Higgs sector consists of five physical Higgs bosons: two neutral scalars, h and H (with $m_h < m_H$ by convention), one neutral pseudo-scalar, A , and a charged pair, H^\pm . At Leading-Order (LO), the coupling of the neutral Higgs bosons to down-type quarks is proportional to $\tan\beta$, where $\tan\beta$ is the ratio of the vacuum expectation values of the two Higgs doublets. This means that the production cross section of a neutral Higgs boson in association with a down-type quark, such as the b -quark, is proportional to $\tan^2\beta$ (again, at LO). Therefore, the $b(h/H/A)$ production mechanism provides a golden mode to search for a neutral Higgs boson at high $\tan\beta$ in the MSSM.

In most of the MSSM parameter phase space, the neutral scalar Higgs bosons h and H decay $\sim 90\%$ of the time into a pair of b -quarks, and $\sim 10\%$ of the time into a pair of τ -leptons. The neutral pseudoscalar A decays into $b\bar{b}$ or $\tau^+\tau^-$ in all of the parameter space, with similar branching ratios ($\sim 90\%$ and $\sim 10\%$, respectively). A search for $bg \rightarrow b(h/H/A) \rightarrow b\bar{b}$ has been previously published by DØ [1]. In this paper, we present a search for the production of a neutral Higgs boson in association with a b -quark, with the subsequent decay of the Higgs boson into two τ -leptons: $bg \rightarrow b(h/H/A) \rightarrow b\tau^+\tau^-$. Although the branching ratio into τ 's is much smaller than the branching ratio into b 's, the τ mode results in a much cleaner signature than the b mode, whereas the latter suffers from a huge heavy-flavor multi-jet background. We perform the analysis using the final state where one τ decays leptonically into a muon ($\tau \rightarrow \mu\nu_\mu\nu_\tau$), and the other τ decays hadronically into a narrow jet ($\tau \rightarrow \tau_h\nu_\tau$, where τ_h denotes the hadronic τ -jet).

II. DATA AND MONTE CARLO SAMPLES

The analysis is performed using data collected by the DØ detector between August 2002 and June 2004 corresponding to an integrated luminosity of 344 pb^{-1} . Two single-muon triggers are used, requiring a Level 2 muon with p_T greater than either 3 or 5 GeV and a Level 3 track with $p_T > 10$ GeV. The total reconstructed luminosity for the selected triggers is 286 pb^{-1} . The average trigger efficiency, measured before event selection and including the geometrical acceptance of the trigger, is $\sim 62\%$.

For the signal simulation, we use the Standard Model process $p\bar{p} \rightarrow bH \rightarrow b\tau^+\tau^-$ in PYTHIA [2], where one of the τ 's is forced to decay leptonically into a muon, whereas the second τ is free to decay to all allowed modes. The QCD multijet and $Z+(b)$ jets backgrounds are estimated from the data. All other backgrounds ($t\bar{t}$, $W+jj$, $W+c\bar{c}$, $W+b\bar{b}$, WW) are simulated using ALPGEN [3] with PYTHIA. PYTHIA minimum bias events are added to all generated events, according to a Poisson distribution with a mean of 0.4 events. The simulated events are processed through the DØ detector and electronics simulation before being reconstructed with the same software as the collider data. They are also weighted by the trigger efficiency parametrization (on an event basis) measured in the data.

III. OBJECT IDENTIFICATION AND SELECTION

There are three types of physics objects used in this analysis: muons, hadronic taus, and jets. All selected objects are required to be associated with the same primary vertex within $\Delta Z_{vtx} < 1$ cm.

Muons are reconstructed from patterns of hits in the muon detectors matched to isolated central tracks, and are required to have $p_T > 12$ GeV.

Hadronically decaying tau's are characterized by a narrow isolated jet with low track multiplicity. We distinguish three τ -types:

1. $\tau^\pm \rightarrow \pi^\pm\nu_\tau$: one track with calorimeter cluster and no associated EM sub-cluster;
2. $\tau^\pm \rightarrow \rho^\pm\nu_\tau \rightarrow \pi^\pm\pi^0\nu_\tau$: one track with calorimeter cluster and at least one associated EM sub-cluster (there can be more than one π^0 in the final state);
3. $\tau^\pm \rightarrow h^\pm h^+ h^-(\pi^0)\nu_\tau$: more than one track, with calorimeter cluster, and with or without associated EM sub-clusters (h refers generically to a hadron).

After an initial selection of τ -candidates based on the calorimeter cluster E_T , sum of the track p_T 's, isolation and width of the tau cone, the candidates are further discriminated against jets using a neural network (NN) which has been trained separately for each τ type. The neural network is the same as the one used for the measurement of the $Z/\gamma^* \rightarrow \tau^+\tau^-$ cross section [4]. The cuts on the NN, however, are optimized for this analysis. For τ -types 1

and 2, τ -candidates are required to have a NN output greater than 0.8. For τ -types 3, because of the larger multijet background, the NN cut is tightened to 0.97.

An event is required to have at least one jet within detector- $|\eta| < 2.5$ and with $E_T > 15$ GeV containing a b -quark. Jets are b -tagged using an algorithm that constructs the jet lifetime from the jet tracks and measures the probability that this lifetime is consistent with a jet originating from a B-meson. The efficiency of the b -tagging algorithm is $\sim 40\%$ for jets of $E_T = 20$ GeV and $|\eta| < 2.5$, with a mistag rate of $\sim 1\%$.

The simulated events are weighted by the ratio of data/simulation of all object identification efficiencies.

IV. BACKGROUNDS

There are three major backgrounds for the $bh \rightarrow b\mu\tau_h$ process. These are QCD multijet production, $Z + (b)jets \rightarrow \mu\tau_h + (b)jets$, and $t\bar{t} \rightarrow b\bar{b}\mu\tau_h$.

A QCD event with three or more jets can have an isolated muon from a misreconstructed jet, a fake τ_h , and a real or fake b -jet. Since the sign of a fake muon is not correlated with the sign of a fake τ_h , the QCD background tends to have equal amounts of opposite sign (OS) and same sign (SS) $\tau\tau$ events. In contrast, the signal should contain only opposite sign $\tau^+\tau^-$ events coming from the Higgs decay. Thus, we require that the reconstructed muon and hadronic tau have opposite charges. The QCD background in this OS sample is estimated from the SS events in the data, in the following steps: first, corrected for the non-QCD background contributions; second, multiplied by the QCD fake rate (measured in a sample of events with a fake muon); third, corrected for a small asymmetry between OS and SS events (also measured from data). Finally, the estimated number of QCD multijet events is multiplied by the b -tagging rate measured in the QCD sample. The latter is between 6-8% for the three τ_h types.

Production of a Z with an associated b -jet is a physical background for the bh process. Both $Z \rightarrow \mu\mu$ (with one muon faking a hadronic tau) and $Z \rightarrow \tau\tau \rightarrow \mu\tau_h$ decays contribute to this background. The b -tagging rate is the same in both cases; therefore, the contribution from these two channels can be estimated together. In addition, light-quark jets associated with a Z can be mistagged as b -jets. The contribution from both real and fake b -jet backgrounds, in either Z decay channel, is estimated by measuring the b -tagging rate in $Z + jets \rightarrow \mu^+\mu^- + jets$ events in the data. This b -tagging rate (2.5%) is then applied to the estimated number of $Z + jets \rightarrow \mu\tau_h + jets$ events in the data.

After b -tagging, the $t\bar{t} \rightarrow \mu\tau_h + b\bar{b}$ is by far the largest background. $t\bar{t}$ events have two high p_T b -jets, a high p_T muon and a high p_T hadronic tau. On the contrary, b -jets in the signal events have relatively low p_T . In order to remove the $t\bar{t}$ background, we use a kinematic neural network (KNN) with four input variables: sum of the E_T 's of all jets in the event (excluding the τ -jet), missing H_T constructed from the jets and selected μ and τ_h , number of jets in the event, and $\Delta\phi$ between μ and τ_h . The background sample used for training was $t\bar{t} \rightarrow \mu\tau_h$ events from a $t\bar{t} \rightarrow l\bar{l}$ sample, which passed all selection cuts except b -tagging. The signal sample used for training was a mixture of $bh \rightarrow b\tau\tau \rightarrow b\mu\tau_h$ events with different Higgs masses, which also passed all cuts except b -tagging. The effect of KNN is tried separately for each τ_h type. Events with type 1 and 3 τ 's do not benefit from KNN; therefore, no cut is used for those types. A cut of $\text{KNN} > 0.4$ is found to be optimal for events with type 2 τ 's (which dominate the final result).

There is also background originating from $W + 2(bc)jets \rightarrow \mu + 2(bc)jets$ and WW production, but this is heavily suppressed by τ -ID and/or by b -tagging. All of these types of background are estimated from Monte Carlo.

V. SYSTEMATIC UNCERTAINTIES

For backgrounds derived from data, the systematic uncertainties result from the statistical uncertainties of the background estimates.

For backgrounds derived from Monte Carlo, the following systematic uncertainties are included in the calculations:

- The Jet Energy Scale uncertainty is estimated by moving the energy scale of all jets in each MC sample (signal and background) by $\pm 1\sigma$, and calculating the new acceptances. Similarly for the Jet Reconstruction Efficiency uncertainty.
- The Tag Rate Function uncertainty is estimated in the same way as the JES uncertainty.
- The τ -identification NN uncertainty is taken from [4].
- The statistical uncertainty of the overall trigger efficiency in the data is used as the muon trigger efficiency systematic uncertainty.
- The luminosity uncertainty is taken to be equal to 6.5%.

- The MC cross sections and their uncertainties are taken as follows:
 - The $t\bar{t}$ cross section is taken from ALPGEN, but the relative uncertainty on it is taken from [5].
 - The W +jets cross section as well as its uncertainty are taken from [6].
 - The WW cross section is taken from ALPGEN and a conservative 15% uncertainty is assigned to it.

VI. CROSS SECTION LIMIT

The estimated number of events from the various backgrounds and the observed number of events in the data for the three τ_h types are shown in Table I. Also shown are the signal acceptance and the number of expected signal events for a Higgs mass of 120 GeV and a $\tan\beta$ value of 80 (as an example).

TABLE I: Signal acceptance (for $M_H = 120$ GeV), expected number of signal events (for $M_H = 120$ GeV and $\tan\beta = 80$), estimated backgrounds and observed number of events for the three hadronic τ types. The QCD and Z +jet backgrounds are estimated from data. The rest of the backgrounds are calculated from Monte Carlo. Quoted uncertainties represent statistical and systematic added in quadrature.

	Type 1	Type 2	Type 3
Signal Accept. (%)	0.15 ± 0.03	0.87 ± 0.11	0.30 ± 0.04
Expected Signal	0.6 ± 0.1	3.5 ± 0.5	1.2 ± 0.2
QCD	0.62 ± 0.22	0.51 ± 0.14	1.45 ± 0.18
Z +jet	0.34 ± 0.09	1.6 ± 0.3	0.35 ± 0.10
$t\bar{t}$ (di- l)	0.18 ± 0.03	0.50 ± 0.11	0.007 ± 0.0013
$t\bar{t}$ (l +jet)	0	0.008 ± 0.008	0.15 ± 0.04
W +jj	0.005 ± 0.005	0.05 ± 0.02	0.40 ± 0.14
W +cc	0.003 ± 0.002	0	0.003 ± 0.003
W +bb	0	0	0.016 ± 0.010
WW	0	0.010 ± 0.002	0.0013 ± 0.0004
Total Background	1.2 ± 0.2	2.6 ± 0.3	2.5 ± 0.2
Observed	0	1	2

Upper limits for the production cross section times branching ratio are set using the modified frequentist approach [7]. In order to maximize the sensitivity, each τ_h type is treated as a separate channel. The differences in shape between signal and background are exploited by using the invariant mass distribution (reconstructed from the 4-vector momenta of the μ , hadronic τ , and missing E_T of the event) of the hypothesized signal, expected background, and observed data in the calculation of the limit. In each channel, the mass distribution is split in three bins: 30-60, 60-85 and 85-180 GeV. The bin size is determined so as to allow enough statistics for the QCD background estimation from the data. Finally, the expected and measured limits are corrected for the branching ratio of $h/H/A \rightarrow \tau^+\tau^-$ (10%), and the branching ratio of one $\tau \rightarrow \mu$ and the other τ decaying hadronically (32%).

Fig. 1 shows the 95% confidence level (CL) expected and observed limits as a function of the Higgs mass. The band indicates the $\pm 1\sigma$ uncertainty on the expected limit. The fact that the observed limit is somewhat outside the 1σ uncertainty of the expected limit is consistent with the mass distribution for type 2 τ_h 's: in this channel, the one observed event appears in the mass bin where we expect the smallest number of events. This results in a larger discrepancy between expected and observed limits than the total number of expected and observed events would indicate. For comparison, Fig. 1 shows also the bh production cross section limit as measured from the $h \rightarrow b\bar{b}$ decay mode [1]. As is evident from the plot, the $h \rightarrow \tau^+\tau^-$ decay mode is competitive with the $h \rightarrow b\bar{b}$ one, despite the 1:9 branching ratio.

VII. INTERPRETATION WITHIN THE MSSM FRAMEWORK

Using the cross section limit for bh production, we can exclude regions of $(m_A, \tan\beta)$ parameter space in the MSSM. Beyond LO, the masses and couplings of the Higgs bosons in the MSSM depend (through radiative corrections) on additional SUSY parameters, besides m_A and $\tan\beta$. Thus, we derive limits on $\tan\beta$ as a function of m_A in two specific scenarios (assuming a CP-conserving Higgs sector): the m_h^{max} scenario (with the parameters $M_{SUSY} = 1000$ GeV, $X_t = 2000$ GeV, $M_2 = 200$ GeV, $\mu = \pm 200$ GeV, $m_g = 800$ GeV) and the no-mixing scenario (with the parameters $M_{SUSY} = 2000$ GeV, $X_t = 0$, $M_2 = 200$ GeV, $\mu = \pm 200$ GeV, $m_g = 1600$ GeV) [8]. The production cross sections,

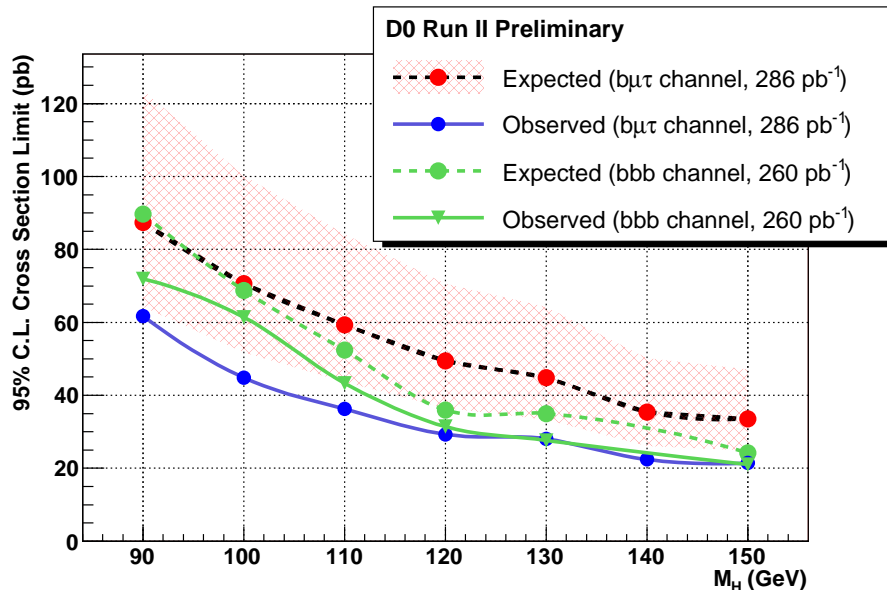


FIG. 1: The 95% C.L. expected and observed limits on the $p\bar{p} \rightarrow bh$ cross section as a function of the Higgs mass, measured from the $\tau^+\tau^-$ and $b\bar{b}$ decay modes. The band indicates $\pm 1\sigma$ uncertainty on the expected limit using the $\tau^+\tau^-$ decay.

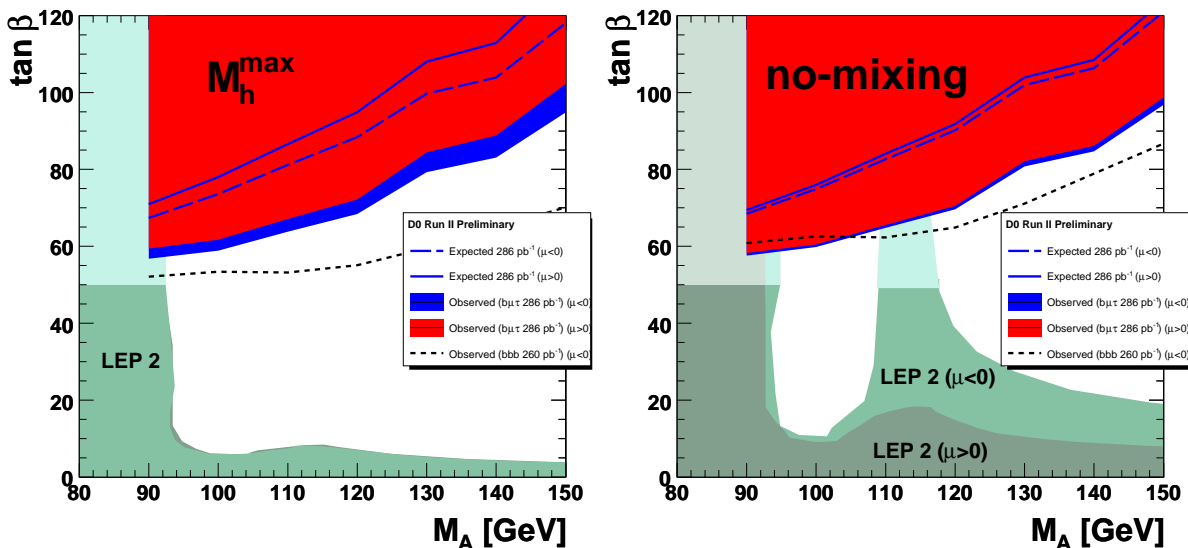


FIG. 2: Excluded region in the $(m_A, \tan\beta)$ plane for the m_h^{max} (left) and the no-mixing (right) scenario of the MSSM, for $\mu = +200$ GeV and $\mu = -200$ GeV. Also shown is the region excluded by the LEP experiments.

widths and branching ratios for the Higgs bosons are calculated over the mass range 90-150 GeV using the FEYNHIGGS program [9]. Since at large $\tan\beta$ the A boson is nearly degenerate in mass with either the h or the H boson, their production cross sections are added. The results are shown in Fig. 2.

This analysis excludes a significant portion of the MSSM parameter space. For negative values of the Higgsino mass parameter μ , the $(h/H/A) \rightarrow \tau^+\tau^-$ decay mode explored here is comparable to the $b\bar{b}$ decay mode, previously published by DØ [1]. For positive values of μ , however, the $\tau^+\tau^-$ mode is superior to the $b\bar{b}$ one, as it does not suffer from the effect of the large supersymmetric radiative corrections to the Higgs decay width, associated with a change of the effective Yukawa couplings of the bottom quarks to the Higgs fields [8]. In general, the $b(h/H/A) \rightarrow b\bar{b}$ channel [1], the $b(h/H/A) \rightarrow b\tau^+\tau^-$ channel presented here, and the inclusive $(h/H/A) \rightarrow \tau^+\tau^-$ channel [10, 11] are all complimentary, since in the regions of the MSSM phase space where the Higgs couplings to b -quarks are enhanced, the couplings to τ -leptons are suppressed, and vice-versa. The combination of all three channels will provide the best

exclusion limits.

-
- [1] DØ Collaboration, V. M. Abazov *et al.*, Phys. Rev. Lett. **95**, 151801 (2005).
 - [2] T. Sjöstrand *et al.*, PYTHIA, Comput. Phys. Commun. **135**, 238 (2001).
 - [3] M. Mangano *et al.*, ALPGEN, JHEP **0307**, 1 (2003).
 - [4] DØ Collaboration, V. M. Abazov *et al.*, Phys. Rev. D **71**, 072004 (2005).
 - [5] N. Kidonakis and R. Vogt, Phys. Rev. D **68**, 114014 (2003).
 - [6] A. Messina, “Measurement of $W^\pm \rightarrow e^\pm \nu$ + Inclusive n-jet Cross Sections with CDF Data at Tevatron Run II”.
 - [7] T. Junk, Nucl. Instrum. Methods Phys. Res. A **434**, 435 (1999).
 - [8] M. Carena, S. Heinemeyer, C.E.M. Wagner and G. Weiglein, Eur. Phys. J. C **45**, 797 (2005).
 - [9] S. Heinemeyer, W. Hollik and G. Weiglein, Phys. Rev. D **58**, 091701 (1998), Phys. Lett. B **440**, 296 (1998).
 - [10] CDF Collaboration, A. Abulencia *et al.*, Phys. Rev. Lett. **96**, 011802 (2006).
 - [11] ”Search for Neutral Higgs Bosons Decaying to tau pairs in $p\bar{p}$ Collisions at $\sqrt{s} = 1.96$ TeV”, DØ Collaboration, V. M. Abazov *et al.*, submitted to Phys. Rev. Lett. (2006); hep-ex/0605009; Fermilab-Pub-06/092-E.